JGP Journal of General Physiology

ARTICLE

Cooperative binding ensures the obligatory melibiose/Na^+ cotransport in MelB

Parameswaran Hariharan and Lan Guan

MelB catalyzes the obligatory cotransport of melibiose with Na^+, Li^+, or H^+. Crystal structure determination of the *Salmonella typhimurium* MelB ($MelB_{St}$) has revealed a typical major facilitator superfamily (MFS) fold at a periplasmic open conformation. Cooperative binding of Na^+ and melibiose has been previously established. To determine why cotranslocation of sugar solute and cation is obligatory, we analyzed each binding in the thermodynamic cycle using three independent methods, including the determination of melting temperature by circular dichroism spectroscopy, heat capacity change (ΔC_p), and regulatory phosphotransferase $EIIA^{Glc}$ binding with isothermal titration calorimetry (ITC). We found that $MelB_{St}$ thermostability is increased by either substrate (Na^+ or melibiose) and observed a cooperative effect of both substrates. ITC measurements showed that either binary formation yields a positive sign in the ΔC_p, suggesting $MelB_{St}$ hydration and a likely widening of the periplasmic cavity. Conversely, formation of a ternary complex yields negative values in ΔCp, suggesting $MelB_{St}$ dehydration and cavity closure. Lastly, we observed that $EIIA^{Glc}$, which has been suggested to trap $MelB_{St}$ at an outward-open state, readily binds to the $MelB_{St}$ apo state at an affinity similar to $MelB_{St}/Na^+$. However, it has a suboptimal binding to the ternary state, implying that $MelB_{St}$ in the ternary complex may be conformationally distant from the $EIIA^{Glc}$-preferred outward-facing conformation. Our results consistently support the notion that binding of one substrate (Na^+ or melibiose) favors $MelB_{St}$ at open states, whereas the cooperative binding of both substrates triggers the alternating-access process, thus suggesting this conformational regulation could ensure the obligatory cotransport.

Introduction

It is well known that cation-coupled secondary active transporters take advantage of the free energy as a form of electrochemical gradient of cations across cellular membranes to move solutes into cells or expel solutes out of cells against the solute electrochemical concentration. The energetically unfavored uptake against a concentration gradient is achieved by the coupled cation moving down its energetically favored electrochemical gradient. The coupling between driving cation and transported solute is obligatory in theory; however, the mechanism underlying the obligation is still enigmatic. From a structural point of view, it is well established that transporters sequentially cycle through many conformations to take solutes from one side of the membrane and release them on the other, and this is attained by opening and closing the solvent-accessing pathway on either side of the membrane alternatively. However, the correlation between alternating-access processes and obligatory coupling is still vague. Here, we applied a thermodynamic approach and ligand-binding assay to study a cation-coupled melibiose transport system and gained insights into the obligatory coupling between Na^+ and melibiose.

Bacterial melibiose permease MelB (Lopilato et al., 1978; Wilson and Ding, 2001) is a member of the glycoside-pentoside-hexuronide:cation symporter family (Poolman et al., 1996), which is a subgroup of the major facilitator superfamily (MFS) transporters (Saier et al., 1999; Guan et al., 2011; Ethayathulla et al., 2014). MelB catalyzes the stoichiometric galactose or galactoside symport with monovalent cation among Na^+, Li^+, and H^+ (Lopilato et al., 1978; Tsuchiya and Wilson, 1978; Bassilana et al., 1985; Wilson and Wilson, 1987; Guan et al., 2011), but it does not select for K^+, Rb^+, or Cs^+ (Guan et al., 2011). Compared with the H^+ coupling, the Na^+-coupled mode exhibits lower K_d and K_m values for melibiose or other galactoside binding and transport, respectively (Niiya et al., 1980; Bassilana et al., 1985; Damiano-Forano et al., 1986; Pourcher et al., 1990; Pourcher et al., 1995; Maehrel et al., 1998; Guan et al., 2011; Hariharan and Guan, 2017). The x-ray 3-D crystal structure of *Salmonella typhimurium* MelB ($MelB_{St}$; Ethayathulla et al., 2014) has shown that its N- and C-terminal six-helix bundles surround a central hydrophilic cavity open to the periplasmic side, and an

Department of Cell Physiology and Molecular Biophysics, Center for Membrane Protein Research, School of Medicine, Texas Tech University Health Sciences Center, Lubbock, TX.

Correspondence to Lan Guan: lan.guan@ttuhsc.edu.

outward-open conformation may be the energetically favorable state of $MelB_{St}$. Residues that play important roles for the binding of galactosides and/or cations are located within the cavity (Mus-Veteau et al., 1995; Pourcher et al., 1995; Mus-Veteau and Leblanc, 1996; Maehrel et al., 1998; Ganea et al., 2001; Wilson and Ding, 2001; Meyer-Lipp et al., 2006; Granell et al., 2010). As previously proposed for other MFS transporters (Abramson et al., 2003; Huang et al., 2003; Kaback, 2015; Yan, 2015), an alternating-access process was also proposed in MelB (Meyer-Lipp et al., 2006; Ethayathulla et al., 2014; Guan, 2018).

Substrate binding is believed to play essential roles for transport. Cooperative interactions of Na^+ and melibiose to $MelB_{Ec}$, a MelB homologue in *Escherichia coli*, was suggested by several biochemical studies (Damiano-Forano et al., 1986; Mus-Veteau et al., 1995; Gwizdek et al., 1997; Ganea et al., 2001; Ganea et al., 2011). With $MelB_{St}$, free energy for individual binding of Na^+ and melibiose or binding of one in the presence of the other was systematically determined with isothermal titration calorimetry (ITC), and a binding thermodynamic cycle has been modeled (Hariharan and Guan, 2017), which clearly shows a positive cooperativity for melibiose and Na^+ binding to $MelB_{St}$. Thus, the binding of either substrate is increased by approximately eightfold in the presence of the other, and the coupling energy is approximately −5 kJ/mol. With regard to the cooperativity between melibiose and H^+, melibiose affords only twofold increases in the H^+ affinity. Clearly, the melibiose coupling efficiency with Na^+ in $MelB_{St}$ is greater than that with H^+. In addition, the H^+ affinity (p*K*a value <6.5, the pH at which the protonation probability is 50%) is not high enough to prepare all MelB protein at a protonated state for transport (Hariharan and Guan, 2017).

The mechanism underlying the cooperativity with MelB is intricate. As an cation-coupled symporter with two types of substrates, a well-regulated mechanism is needed to prevent ion leak; however, the mechanism in place for this regulation is still poorly understood. To address this fundamental question, in this study, we intended to correlate substrate binding and conformational changes using three different methods to examine each step of the thermodynamic cycle of Na^+ and melibiose binding to $MelB_{St}$. This includes the analyses of hydration/dehydration processes by determining the heat capacity change (ΔC_p), the substrate effect on temperature-dependent denaturation using circular dichroism (CD) spectroscopy, and binding of a conformational binder phosphotransferase $EIIA^{Glc}$ to $MelB_{St}$. $EIIA^{Glc}$ is a central regulator in the glucose-specific phosphoenolpyruvate/sugar phosphotransferase system (PTS) in certain bacteria (Meadow and Roseman, 1982), and it is a useful tool to probe conformational changes of those regulated transporters (Hariharan and Guan, 2014). All data stemming from the three independent tests consistently argue for a simple correlation; thus, with binding of one substrate (either Na^+ or melibiose), $MelB_{St}$ favors open conformations (likely outward facing), whereas the cooperative binding of both substrates induces cavity closure. Thus, cooperative binding is the key that regulates the alternating-access process and ensures the obligatory cotransport as the core mechanism for symport.

Materials and methods

Reagents

All chemicals used in this study were of analytical grade and purchased from standard commercial suppliers. The detergent undecyl-β-D-maltopyranoside (UDM) and n-dodecyl-β-D-maltopyranoside (DDM) were purchased from Anatrace.

Buffers

For ITC measurement, we used a buffer consisting of 20 mM Tris-HCl, 50 mM choline chloride (ChoCl), 0.035% UDM, and 10% glycerol, pH 7.5 (referred to as "main buffer" in this article), which is a Na^+-free and ligand-free buffer. For CD measurement, the buffer is consisting of 10 mM KPi, pH 7.5, 0.035% UDM, and 10% glycerol. Specific components such as salt and/or melibiose were supplemented as defined. Concentrated stock solutions of 4 M NaCl and 1 M melibiose were prepared by directly dissolving them in the main buffer and kept at −20°C. Notably, $MelB_{St}$ at pH 7.5 has <20% populations at a protonated form (Hariharan and Guan, 2017). Since $MelB_{St}$ protonation exhibits only an approximately twofold effect on the sugar affinity, the information stemming from the main buffer condition might mainly represent the apo state; for simplification, $MelB_{St}$ in this condition is referred as apo $MelB_{St}$.

Overexpression of $MelB_{St}$ and affinity purification

Overexpression of the WT and single-site mutant D55C $MelB_{St}$ was performed in *E. coli* DW2 cells (*mel*A$^+$, *mel*B, and *lac*ZY) from a constitutive expression plasmid pK95ΔAH/$MelB_{St}$/$CHis_{10}$ (Pourcher et al., 1995; Guan et al., 2011) by fermentation as described previously (Amin et al., 2014). The cells were grown in Luria–Bertani broth supplemented with 50 mM KPi, pH 7.0, 45 mM $(NH_4)SO_4$, 0.5% glycerol, and 100 mg/liter ampicillin. The protocols for membrane preparation and $MelB_{St}$ purification by cobalt-affinity chromatography after extraction in a detergent UDM have been described previously (Ethayathulla et al., 2014). $MelB_{St}$ protein samples were dialyzed against the main buffer as defined above, concentrated with a Vivaspin column at a 50-kD cutoff to 20–50 mg/ml, and stored at −80°C after flash-freezing with liquid nitrogen.

Overexpression of unphosphorylated IIA^{Glc}

The overexpression of *E. coli* $EIIA^{Glc}$ at unphosphorylated form was performed as described previously (Hariharan and Guan, 2014). The glucose-specific phosphotransferase $EIIA^{Glc}$ is a component of PTS, and only the unphosphorylated form binds MelB and other permeases. Briefly, *E. coli* BL21 DE3 containing a T7-based expression plasmid p7XNH3/IIA-NH10 encoding *E. coli* $EIIA^{Glc}$ with a N-terminal 10-His tag and a linker containing HRV-3C protease cleavage site (MHHHHHHHHHHLEVLFQGPS) was used for overexpression. To ensure the $EIIA^{Glc}$ at an unphosphorylated form, transformants were passaged in the LB media supplemented with 0.2% D-glucose, 0.5% glycerol, and 50 mg/liter of kanamycin thrice and then diluted into 2 liters of the same media. $EIIA^{Glc}$ protein expression was induced with 0.2 mM IPTG at a cell density of absorbance $(A)_{600}$ = 0.8 for 4 h. The unphosphorization status of purified $EIIA^{Glc}$ produced by this method was previously confirmed by phos-tag staining

analyses (Hariharan and Guan, 2014) and with alkaline phosphatase treatment (New England BioLabs, Inc.).

Affinity purification of EIIA^{Glc}

EIIA^{Glc} purification by cobalt-affinity chromatography using Talon resin (Clontech) was performed as described previously (Hariharan and Guan, 2014). The purified EIIA^{Glc} samples were dialyzed against the main buffer supplemented with 20 mM NaCl, concentrated with a Vivaspin column at a 10-kD cutoff to ∼50–100 mg/ml, and stored at −80°C after flash-freezing with liquid nitrogen. Prior to application, the concentrated solution of EIIA^{Glc} protein were further dialyzed against the main buffer and then used for sample preparation containing specific compositions.

Overexpression and purification of membrane scaffold protein (MSP)

Overexpression of MSP1D1E3 with N-terminal 7-His tag followed by spacer sequence and tobacco etch virus (TEV) protease cleavage site (mass 32.6 kD) was performed by a plasmid pMSP1E3D1 (Addgene; #20066) in the *E. coli* BL21 (DE3) strain. MSP1D1E3 yields nanodiscs with a diameter of ∼12.1 nm (Ritchie et al., 2009). The cells were grown in LB media containing 0.5% glucose and 30 mg/liter kanamycin at 37°C; 1 mM IPTG was added at an A_{600} of ∼0.6 for another 2.5 h. The MSPs from the cell lysates were purified with metal-affinity purification using INDIGO Ni-Agarose (Cube Biotech). The eluted MSPs at 300 mM imidazole were dialyzed at 4°C against 20 mM Tris-HCl, pH 7.5, and 100 mM NaCl and concentrated to ∼8 mg/ml. The His tag on MSP was removed by His-tagged TEV protease at 1:20 (TEV/MSP, mol/mol) in the same buffer. Processed MSP proteins were separated from the His-tagged TEV protease and remaining unprocessed His-tagged MSP by Ni-agarose chromatography as a flowthrough, concentrated to ∼6–8 mg/ml, frozen in liquid nitrogen, and stored at −80°C.

Reconstitution of MelB$_{St}$ into phospholipid bilayer nanodiscs

A stepwise reconstitution method was adapted from the reported protocols (Zoghbi et al., 2016). Briefly, 1 mg of the purified MelB$_{St}$ in UDM at 1 mg/ml was mixed with 5.2 mg *E. coli* polar lipids extract from a stock of 40 mg lipids/ml in DDM, yielding a protein:lipid ratio of 1:350 (mol/mol) or 1:5.6 (mg/mg). The protein/lipid mixture was incubated for 10 min on ice; MSP1D1E3 protein was added at a 5:1 molar ratio of MSP1D1E3:MelB$_{St}$, followed by incubation at 23°C with mild stirring for 30 min. The detergents were removed using Bio-Beads SM-2 (500 mg beads per 1 mg MelB$_{St}$) with mild stirring at 4°C for 2 h, followed by overnight incubation after adding another portion of Bio-Beads SM-2 (300 mg). The reconstituted phospholipid bilayer nanodiscs were collected using a 22-gauge needle and centrifuged at 20,000 *g* for a few minutes at 4°C to remove the residual Bio-Beads SM-2. Reconstituted nanodiscs containing His-tagged MelB$_{St}$ in the supernatant that may also contain empty nanodiscs were further isolated by metal-affinity purification using Ni-NTA beads. The elute containing MelB$_{St}$ in nanodiscs was further dialyzed against a ligand-free main buffer without detergent. The reconstituted nanodiscs have a MelB$_{St}$/MSP1D1E3 stoichiometry of 1:2, and protein concentration was measured at A_{280} nm with a calculated extinction coefficient (ε = 135110) based on 1 MelB$_{St}$ and 2 MSP1D1E3 molecules. This extinction coefficient was verified by SDS-15%PAGE and Micro BCA assay. The MelB$_{St}$ lipid nanodiscs were aliquoted, flash-frozen in liquid nitrogen, and stored at −80°C.

Protein assay

The Micro BCA Protein Assay (Pierce Biotechnology, Inc.) was used as the protein concentration assay.

CD spectroscopy

CD measurements were performed using a Jasco J-815 spectrometer equipped with a Peltier MPTC-490S temperature-controlled cell holder unit. MelB$_{St}$ at 10 µM in 10 mM KPi, pH 7.5, 10% glycerol, and 0.035% UDM in the absence or presence of 50 mM KCl or NaCl and/or melibiose at 50 mM was prepared by an ∼100-fold dilution of concentrated MelB$_{St}$ in the main buffer. An aliquot of 200-µl MelB$_{St}$ sample was placed in a 1-mm quartz cuvette on the temperature-controlled cell holder. CD spectra for a wavelength range of 200–260 nm were collected at a data pitch of 0.1 nm using a bandwidth of 1 nm and scanning speed of 100 nm/min with Jasco Spectra Measurement software (version 2). Each spectrum was corrected by subtracting the corresponding buffer in the absence of MelB$_{St}$.

Melting temperature (T_m) determination

Thermal denaturation tests were performed at temperatures between 25°C and 80°C for each ligand condition. Ellipticity at 210 nm was recorded at a 1°C interval with the temperature ramp rate at 1°C per minute. The ellipticity at 210 nm was plotted against temperature, and the T_m value was defined as the temperature leading to a half-maximal decrease in ellipticity, which was determined by fitting the data to the Jasco Thermal Denaturation Multi Analysis Module.

ITC measurements

All ligand-binding assays were performed with TA Instruments (either a Nano-ITC device with an effective sample cell volume of 163 µl or an Affinity-ITC with an effective sample cell volume of 185 µl). In a typical experiment, the titrands (MelB$_{St}$) in the ITC sample cell were titrated with the specified titrants, the ligand, (placed in the Syringe) by an incremental injection of 2-µl aliquots at an interval of 300 s at a constant stirring rate of 250 rpm (Nano-ITC) or 125 rpm (Affinity-ITC). All testing samples were degassed using a TA Instruments Degassing Station (model 6326) for 15 min before titration.

Na^+ binding was measured in the absence or presence of melibiose at 15°C, 20°C, 25°C, or 30°C. A solution containing 5 mM or 2 mM NaCl in the absence or presence of 50 mM melibiose, respectively, was prepared by a dilution from stock solutions and injected into the ITC sample cell prefilled with MelB$_{St}$ in the main buffer at a concentration of ∼80 µM with or without melibiose at 50 mM. Heat changes were collected at a given temperature under an identical titration protocol as described above. For each assay, the system was preequilibrated to the defined temperature.

Melibiose binding was measured in the absence or presence of Na^+ at 15°C, 20°C, 25°C, 30°C, or 35°C. A solution of 80 mM or 10 mM melibiose in the absence or presence of NaCl at 100 mM prepared from the stock solutions was injected into the ITC sample cell containing $MelB_{St}$ at 80 µM with or without NaCl at 100 mM. Heat changes were collected at a given temperature under an identical titration protocol.

$EIIA^{Glc}$ binding to $MelB_{St}$ in UDM or reconstituted nanodiscs was measured at 25°C. The concentrated $EIIA^{Glc}$ sample in the 20 mM NaCl–containing base-buffer was changed to Na^+-free main buffer by dialysis against a large volume of main buffer and then used to prepare the testing solution at a concentration of 435 or 600 µM supplemented with one of the components (50 mM ChoCl, 50 mM NaCl, or 50 mM melibiose) or two components (50 mM NaCl and 50 mM melibiose). For binding to the $MelB_{St}$ nanodiscs in all four conditions, $EIIA^{Glc}$ at a concentration of 245–280 µM was used. $MelB_{St}$ in UDM or in nanodiscs were buffer-matched to defined buffer conditions, placed in the ITC sample cell, and titrated with $EIIA^{Glc}$ in corresponding buffers.

ΔC_p was determined by plotting the measured enthalpy change (ΔH) at different temperatures and fitting the data to a linear function. The sign and value of ΔC_p directly resulted from the slope ($\Delta C_p = \Delta H/\Delta T$). If ΔH makes more contribution to the binding free energy along with the increase in temperature, then the sign ΔC_p is negative, and vice versa.

ITC data processing was performed with NanoAnalyze software (version 3.6.0), which was provided with the ITC equipment. The normalized heat changes or total heat changes were subtracted from the heat of dilution elicited by last few injections, where no further binding occurred, and the corrected heat changes were plotted against the molar ratio of titrant versus titrand. The values for the binding association constant (K_a) and ΔH were determined by fitting the data with a one-site independent-binding model. In all cases, the binding stoichiometry (N) number was fixed to 1, since it is a known parameter, which can restrain the data fitting and achieve more accurate results (Turnbull and Daranas, 2003). All other thermodynamic parameters were calculated by the following equations: the binding free energy (ΔG) = $-RT \ln K_a$, where R is the gas constant (8.315 J/mol·K) and T is the absolute temperature; $\Delta G = \Delta H - T\Delta S$; the entropy change ($-T\Delta S$) = $\Delta G - \Delta H$; dissociation constant (K_d) = $1/K_a$.

The obtained reaction entropy is a sum of three major components: $\Delta S_{Sum} = \Delta S_{Mix} + \Delta S_{Solv} + \Delta S_{Conf}$. ΔS_{Sum} can be calculated as described above. ΔS_{Mix} is a known parameter that can be calculated (Zakariassen and Sorlie, 2007), reflecting the mixing of solute and solvent molecules. This entropy change is derived from the changes in translational/rotational degrees of freedom of these molecules. Based on the bimolecular binding reaction at 1 M standard state, $\Delta S_{Mix} = R \ln (1/55.5) = -33$ J/mol·K. Since the entropy of polar and apolar solvation is close to zero at a temperature of near 385°K, the solvent entropy change at 25°C is given as $\Delta S_{Solv} = \Delta C_p \ln (298.15/385.15)$; Zakariassen and Sorlie, 2007). ΔC_p of the binding can be obtained by fitting ΔH versus temperature. $\Delta S_{Conf} = \Delta S_{Sum} - \Delta S_{Mix} - \Delta S_{Solv}$.

Statistical analysis

An unpaired t test was used for data analysis. P values <0.05 were considered statistically significant.

Results

Substrate effects on $MelB_{St}$ thermostability

It has been shown previously that $MelB_{St}$ in detergent UDM binds Na^+ and melibiose at affinities similar to that measured with native right-side-out bacterial membrane vesicles (Guan et al., 2011; Amin et al., 2014; Amin et al., 2015; Hariharan and Guan, 2017), indicating that UDM is a suitable detergent for functional studies of $MelB_{St}$ in solutions.

CD spectroscopy and thermal denaturation have been used to analyze the stability of $MelB_{St}$ proteins purified from various strains with genetically modified lipid environments (Hariharan et al., 2018), and no obvious differences in CD spectra and T_m were obtained. In this study, we analyzed potential substrate effects on $MelB_{St}$ thermostability. Overall, the CD spectra in the absence or presence of substrates were undistinguishable, with a profile typical of α-helical-dominant proteins (Fig. 1 a), featuring strong negative ellipticity submaxima at 209 nm and 222 nm. Thermal denaturation tests were performed at temperatures between 25°C and 80°C or 100°C, as described in Materials and methods (Fig. 1 a). The ellipticity changes at 210 nm, which is more stable and sensitive to the α-helical contents, were recorded at a 1°C interval. All consistently show that the unfolded fractions increase as the temperature increases, yielding sigmoidal curves. The data support a two-state unfolding model, where transition of the folded native state to a fully unfolded state occurs via a single cooperative process. Under all conditions, the melting temperatures, at which 50% protein unfolded, range from 53°C to 56°C depending on the protein buffer composition (Fig. 1 b and Table 1). The stability for $MelB_{St}$ in the apo state is fairly good, with a T_m value of 53°C, which is similar to that obtained in the presence of the control cation, K^+, which is not recognized by MelB (Guan et al., 2011). Na^+ or melibiose alone slightly increases T_m, but binding of cosubstrate significantly elevates the T_m to 56.71°C, which is 3.43°C higher than that at the apo state and 1.12°C greater than the sum of the increase gained from an individual substrate (Table 1). Thus, positive cooperativity of the two substrates on $MelB_{St}$ thermostability exist; notably, the equilibrium binding of the cosubstrates to $MelB_{St}$ is also positively cooperative (Hariharan and Guan, 2017).

Unexpectedly, a nonspecific salt effect on $MelB_{St}$ denaturation was observed above 60°C (Fig. 1 b). In the presence of either the substrate Na^+ or the nonsubstrate K^+, denaturation is completed at 4–5°C faster than that in the absence of salt. Melibiose affords no protection at this high range of temperatures. To further analyze the Na^+ effect on MelB stability, a well-studied mutant with a single Cys replacement at position D55 (D55C), which abolishes the MelB Na^+ binding (Hariharan and Guan, 2017), was used to clarify the possibly specific and/or nonspecific effects of Na^+ to $MelB_{St}$ thermal stability. The apo state of D55C mutant is more thermo stable, because the course of thermal denaturation in the absence of salt is dramatically

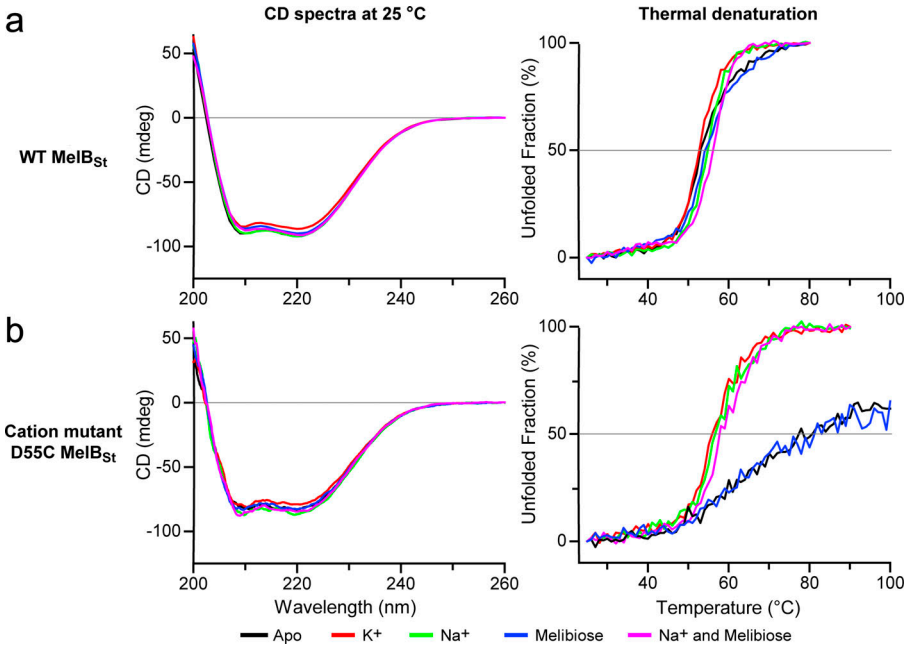

Figure 1. **CD spectroscopy.** $MelB_{St}$ samples at a protein concentration of 10 µM in the CD assay buffer (10 mM KPi, pH 7.5, 10% glycerol, and 0.035% UDM) in the absence or presence of a salt and/or melibiose at 50 mM were prepared for CD measurements as described in Materials and methods. Left: Far-UV CD spectra. The presented spectra were recorded between 200 and 260 nm at 25°C after subtracting from each the corresponding buffer control. mdeg, millidegree. Right: Thermal denaturation. The CD ellipticity changes were recorded at 210 nm at a 1°C interval, with the temperature ramping up at 1°C per minute, and are expressed as a percentage of the unfolded fraction. **(a)** WT $MelB_{St}$. **(b)** D55C $MelB_{St}$ mutant. The color legends indicate the assay conditions.

slower than that in WT. Interestingly, the completion of denaturation cannot be reached, even at 100°C, yielding an estimated T_m >80°C. As expected, the T_m increase by Na^+ does not exist with this cation site–compromised mutant; instead, Na^+ promotes $MelB_{St}$ denaturation as K^+ does, exhibiting a nonspecific salt effect at high temperatures. Melibiose slightly increases the stability by 1.4°C (Table 1). Therefore, in the WT with an intact Na^+ site, the Na^+ binding–exerted stabilizing effect at temperatures around T_m is strong, which prevents the occurrence of a nonspecific salt effect, but at higher temperatures, the nonspecific denaturation effect dominates. Thus, in $MelB_{St}$, Na^+ plays a dual role in the thermal denaturation process.

ΔC_p of $MelB_{St}$ complex formation in the binding thermodynamic cycle by ITC

Thermal denaturation tests revealed that $MelB_{St}$ is stable in the absence of a substrate, with a T_m of >53°C, which allows us test the substrate binding at elevated temperatures. As reported previously, we have determined the binding affinity at each step of the binding thermodynamic cycle in MelB (Hariharan and Guan, 2017). In this article, we determined ΔC_p at each step by ITC measurements to scrutinize the underlying thermodynamic mechanisms.

All thermograms obtained are exothermic (Fig. 2) with positive peaks. The cumulative heat changes derived from each peak were plotted against a molar ratio of titrant (Na^+ or melibiose)/titrand ($MelB_{St}$), and all curves fit reasonably well to an independent one-binding-site model. All binding parameters were determined as described in Materials and methods. The ΔC_p sign and value ($\Delta H/\Delta T$) were determined by a linear fitting from an enthalpy–temperature plot. While a single binding isotherm could potentially provide full thermodynamic parameters, the shape of binding curve needs to be at least sigmoidal with multiple points on the slope. It is often found that most biomolecular interactions with lower affinities are less likely to meet these requirements, but the binding affinity (K_a, K_d, and ΔG) could be determined accurately in most cases. In this study, while accurate determination of enthalpy values from either binding is not feasible, the trend of enthalpic change in response to temperature (i.e., the sign of ΔC_p term) is reliable, even if the value of ΔC_p cannot be accurately determined. ΔC_p contains rich insights into the intricate thermodynamics and mechanisms; briefly, a positive or negative sign indicates hydration or dehydration as the predominant process.

Melibiose binding to apo $MelB_{St}$ and temperature dependence

The apo $MelB_{St}$ in the main buffer was titrated with melibiose at 15°C, 20°C, 25°C, and 30°C. Similar values on the binding free energy ΔG (−11.27 to −10.81 kJ/mol) or K_d (9–13 mM) were obtained, indicating that the binding affinity is not dramatically affected at this range of temperatures (Figs. 2 and 3; Table 2). The thermograms (Fig. 2), however, clearly show that the amount of heat release is temperature dependent; at lower temperatures, more heat is released than that at higher temperatures, which is shown as higher peaks on the thermograms. Given that ΔG is at similar values, the higher peaks at lower temperatures directly indicate that an enthalpic contribution to ΔG is greater at lower temperatures than at higher temperatures (from −25.91 kJ/mol at 15°C to −16.40 kJ/mol at 30°C; $\Delta\Delta H$ of nearly 10 kJ/mol; Table 2). The enthalpic change is greater than ΔG to compensate for the entropic loss; thus, enthalpy and entropy compensation yields a similar value in ΔG. Along with the increase in temperature, entropy becomes more favorable to ΔG. At the full temperature range, ΔH makes a sole favorable contribution to the ΔG.

Na^+ binding to apo $MelB_{St}$ and temperature dependence

$MelB_{St}$ in the main buffer was also used for the Na^+-binding assay at 15°C, 20°C, 25°C, and 30°C, which reveals that the Na^+-binding affinity is also independent of temperature (Table 2),

Table 1. **Thermal denaturation**

$MelB_{St}$	Buffer[a]	Number of tests	10% unfolding (°C)	90% unfolding (°C)	50% unfolding (Tm, °C)	ΔTm (°C; P value)
WT	Apo	3	46.13 ± 0.70[b]	62.26 ± 0.50	53.29[c] ± 0.05	/
	K^+	2	46.06 ± 0.02	59.94 ± 0.69	53.34 ± 0.04	0.05[d] (>0.05[e])
	Na^+	3	49.07 ± 0.28	60.06 ± 0.29	54.83 ± 0.03	1.54 (<0.05)
	Mel	2	45.95 ± 0.47	64.24 ± 0.42	54.07 ± 0.07	0.78 (<0.05)
	Mel and Na^+	2	49.42 ± 0.13	61.76 ± 0.09	56.71 ± 0.05	3.43 (<0.05)
D55C	Apo	2			>80[f]	
	K^+	2	46.51 ± 0.71	65.07 ± 0.06	56.15 ± 0.16	>14
	Na^+	3	46.35 ± 0.25	66.51 ± 0.31	56.75 ± 0.25	>14
	Mel	2			>80	
	Mel and Na^+	2	46.25 ± 0.20	68.52 ± 0.27	58.15 ± 0.11	1.40 (<0.05)

[a]CD assay buffers consisted of 10 mM KPi, pH 7.5, 10% glycerol, and 0.035% UDM with a given component at 50 mM of each.
[b]SEM.
[c]T_m value at which 50% protein unfolded.
[d]The difference in T_m value when compared with apo (in WT) or the buffer containing Na^+ (in D55C mutant).
[e]Unpaired *t* test; $P < 0.05$ was considered statistically significant.
[f]Completion of denaturation cannot be approached, so this value is an estimation based on the unfolded fraction.

with a ΔG of −17 to −18 kJ/mol or K_d of 0.5 −0.7 mM. Interestingly, a similar temperature dependence in ΔH as described for melibiose binding to apo $MelB_{St}$ was also obtained, even with greater dependence. From 15°C to 30°C, the enthalpy decreases from −35.75 kJ/mol to −16.02 kJ/mol ($\Delta\Delta H$ of nearly 20 kJ/mol). As compensation, the entropy force becomes less unfavorable, and at 30°C, it even makes a small contribution to the favorable ΔG.

The enthalpy–temperature plots in both cases exhibit a linear function. The sign and slope from a linear fitting are the sign and value of ΔC_p (Fig. 3). When melibiose binds to the apo $MelB_{St}$, a positive sign of ΔC_p of 643.01 ± 26.92 J/mol·K was obtained; when Na^+ binds to the apo $MelB_{St}$, the sign of ΔC_p was also positive, with a greater value of 1,305.20 ± 50.63 J/mol·K.

Melibiose or Na^+ to $MelB_{St}$ binary and temperature dependence

ITC measurements with $MelB_{St}$ preincubated with 50 mM of Na^+ or melibiose were performed at 15°C, 20°C, 25°C, 30°C, or 35°C. The binding affinity for either substrate is largely improved compared with the binding at the apo state; the increases are approximately eightfold or −5 kJ/mol across the full range of temperatures, further confirming cooperative binding, as previously reported from data collected at 25°C. The favorable ΔG values at most temperatures were driven by both enthalpy and entropy, which was largely different from the binary formation, where the enthalpy term was the sole or major driving force. In other words, entropy increases and makes more favorable contributions to ΔG in the ternary formation than in the binary formation. Consistently, there is no temperature dependency in binding affinity; remarkably, negative values of ΔC_p in both cases were obtained (Fig. 3 and Table 2; −424.93 ± 40.78 J/mol·K or −760.50 ± 33.18 J/mol·K for melibiose or Na^+ binding to corresponding binary states, respectively).

These studies show that negative ΔC_p values were derived from the formation of a ternary complex (regardless of the binding order), which is opposite to the positive ΔC_p values from formation of each binary complex. The data strongly indicate that the thermodynamic mechanisms underlying the two types of binding (binary and ternary) are dramatically different.

Parameterization of entropy change

As the free energy remains nearly constant across temperatures from 15°C to 30°C or 35°C, temperature-dependent entropy changes point in an opposite direction compared with the temperature-dependent ΔH (Fig. 3). The binding entropy and enthalpy exhibit perfect compensation. The obtained reaction entropy change ($-\Delta S_{Sum} = -T\Delta S/T$) is the sum of the solvent entropy ($-\Delta S_{Solv}$), conformational entropy ($-\Delta S_{Conf}$), and mixing entropy (ΔS_{Mix}). The solvent entropy can be estimated from the binding heat capacity ($\Delta S_{solv} = \Delta C_p \ln 298.15/385.15$ or $-\Delta S_{solv} = 0.256 \cdot \Delta C_p$) as described in Materials and methods, the mixing entropy is known, so all major contributors to the overall reaction entropy, ΔS_{Sum}, can be parameterized. Thus, the missing information on conformational entropy or thermal motion entropy can be calculated (Table 3).

The positive values in $-\Delta S_{Sum}$ for melibiose or Na^+ binding to apo $MelB_{St}$ result in positive values in solvent entropy ($-\Delta S_{Solv}$) of 164.61 J/mol·K or 334.13 J/mol·K, respectively (Table 3), which indicate that hydration processes dominate when either substate binds to apo $MelB_{St}$. In both cases, the conformational entropy makes favorable contributions to the total entropy changes.

When melibiose or Na^+ binds to $MelB_{St}$ binary states to form ternary states, $-\Delta S_{Sum}$ has a negative sign, implying that favorable ΔG was also driven by the entropic change in addition to the enthalpic change (Table 2). The solvent entropy change makes the sole favorable contribution to $-\Delta S_{Sum}$, with a large negative value of −108.78 or −194.56 J/mol·K for melibiose or Na^+ binding to the binary, respectively (Table 3). The data indicate that a major dehydration process associates with Na^+ or

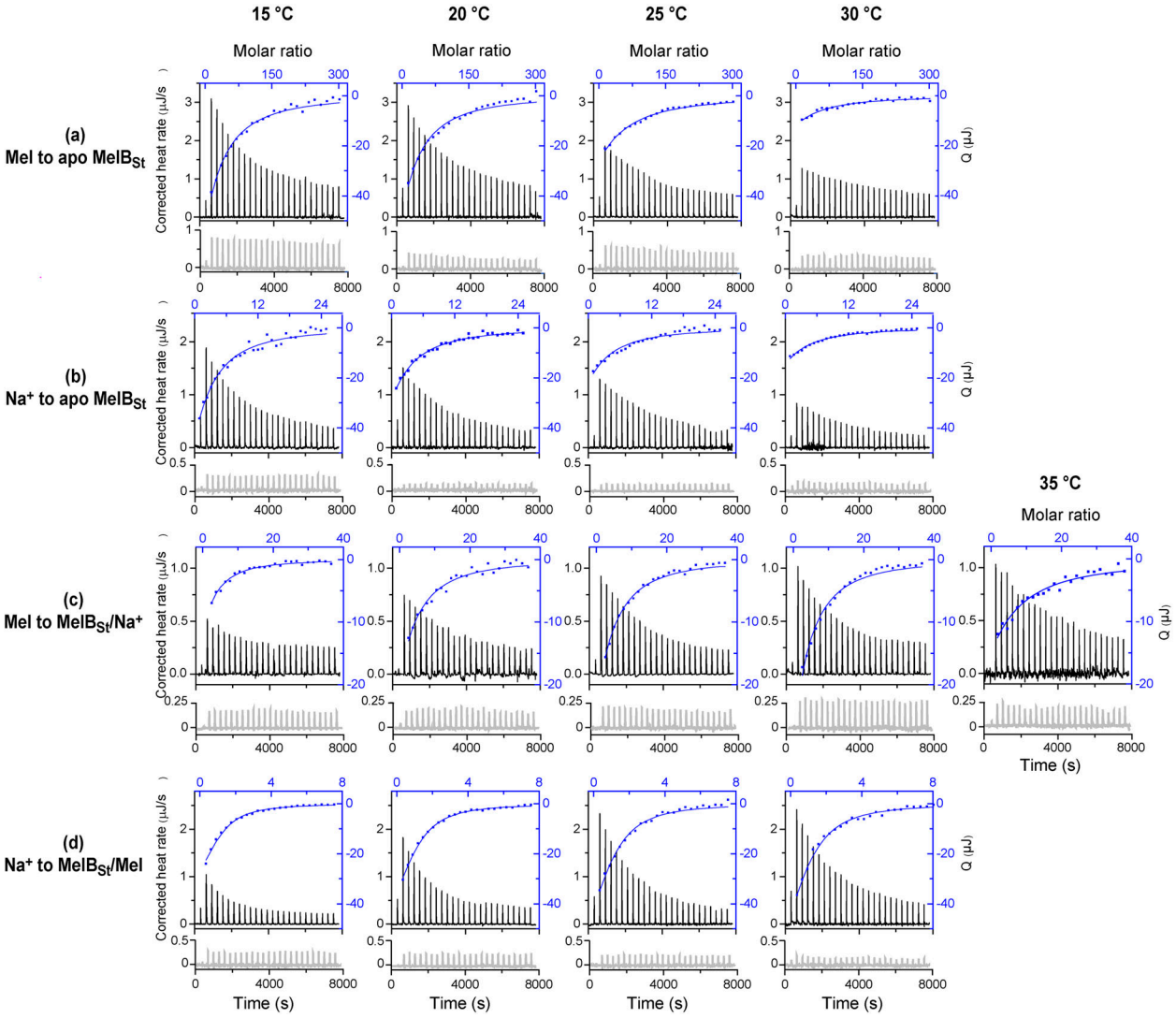

Figure 2. **Measurements of substrate binding to $MelB_{St}$ by ITC and temperature dependence.** Heat changes from substrate binding to $MelB_{St}$ were collected with ITC calorimeters (TA Instruments) at 15°C, 20°C, 25°C, 30°C, or 35°C, respectively. For each measurement, an aliquot of 80 μM $MelB_{St}$ in the ligand-free main buffer (20 mM Tris-HCl, pH 7.5, 50 mM ChoCl, 0.035% UDM, and 10% glycerol) without addition (apo $MelB_{St}$) or with addition of 100 mM NaCl or 50 mM melibiose (the binary complex) was placed in the sample cell. Melibiose or NaCl solution prepared in matching buffers was placed in the syringe and incrementally injected with 2-μl aliquots into the sample cell at a 300-s interval as described in Materials and methods. **(a)** Melibiose binding to Apo $MelB_{St}$. Melibiose at 80 mM was titrated to the main buffer with $MelB_{St}$. **(b)** Na^+ binding to apo $MelB_{St}$. NaCl at 5 mM was titrated in $MelB_{St}$ in the main buffer. **(c)** Melibiose binding to $MelB_{St}/Na^+$ binary complex. Melibiose at 10 mM was titrated in $MelB_{St}$ in the main buffer with addition of 100 mM NaCl. **(d)** Na^+ binding to $MelB_{St}$/Mel binary complex. NaCl solution at 2 mM was titrated to $MelB_{St}$ in the main buffer with addition of 50 mM melibiose. For the determination of the temperature dependence, each measurement was performed under identical testing protocols, including identical buffer compositions and fixed concentrations for ligands (titrant) and protein (titrand), as well as the ITC measurement settings. The thermogram was plotted as the baseline-corrected heat rate (μJ/s; left axis) versus time (bottom axis) for the titrant to $MelB_{St}$ (black) or buffer (gray) under an identical scale. The heat change *Q* (μJ; filled blue symbol) was plotted against the ligand/$MelB_{St}$ molar ratio based on the top/right axes. The binding isotherm was obtained by fitting the data using the one-site independent-binding model included in the NanoAnalyze software (version 3.6.0). The binding stoichiometry *N* number was fixed to 1 in all cases. The determination of thermodynamic parameters was determined as described in Materials and methods, and the number of tests is presented in Table 2.

melibiose binding to form the $MelB_{St}$ ternary complex. In both cases, the conformational entropy is unfavorable.

Probing conformational changes with the physiological regulator $EIIA^{Glc}$

The glucose-specific phosphotransferase $EIIA^{Glc}$ of the bacterial phosphoenolpyruvate/carbohydrate PTS is the central regulator allowing certain bacteria to use the favorable energy source glucose preferentially (Meadow and Roseman, 1982). The protein $EIIA^{Glc}$, a small and rigid cytosolic protein with a mass of 18.1 kD, is a conformational binder, which binds more than a dozen non-PTS sugar transporters belonging to various families (e.g., MFS transporters and ABC transporters), as well as several types of soluble enzymes, and regulates their activities in the catabolite repression (Deutscher et al., 2014). We have shown that the unphosphorylated $EIIA^{Glc}$ stoichiometrically binds to

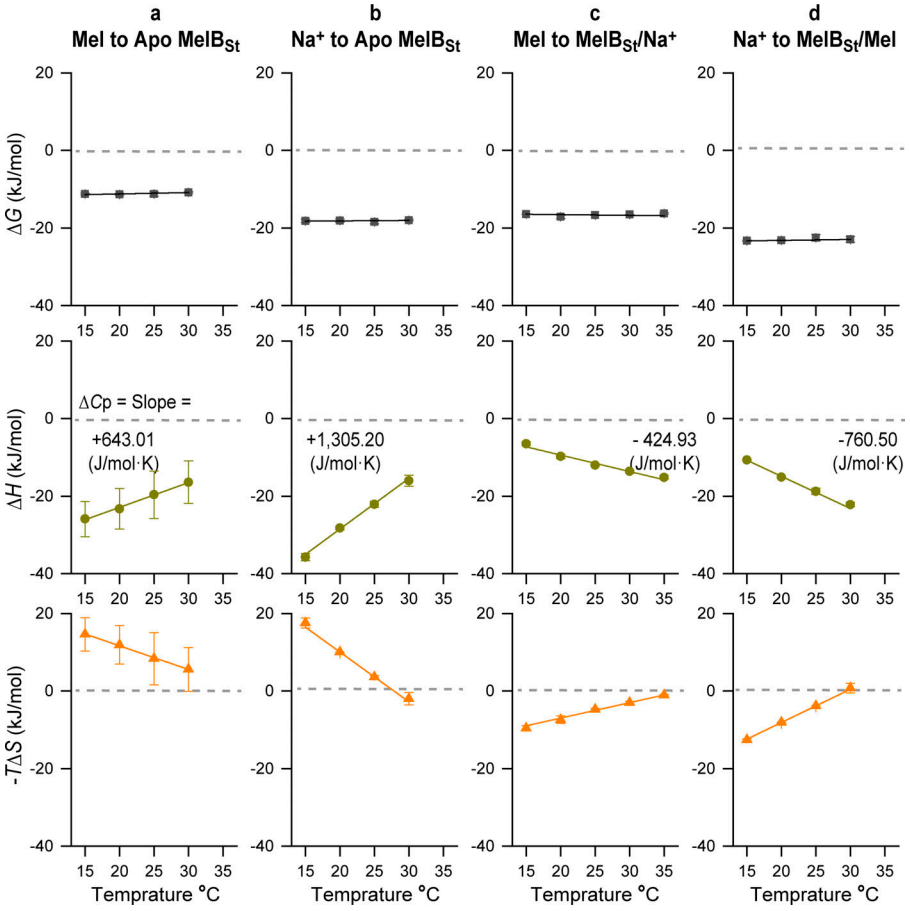

Figure 3. **Enthalpy–entropy compensation and determination of ΔC_p.** The binding free energy change ΔG, ΔH, and entropy change $-T\Delta S$ at each temperature presented in Table 2 were individually fit into a linear function. The sign and value for each ΔC_p were obtained from ΔH versus temperature fit as indicated. **(a)** Melibiose binding to $MelB_{St}$ in the main buffer (the apo $MelB_{St}$). **(b)** Na^+ binding to the apo $MelB_{St}$. **(c)** Melibiose binding to $MelB_{St}$ preequilibrated with NaCl at 100 mM ($MelB_{St}/Na^+$ binary complex). **(d)** Na^+ binding to $MelB_{St}$ preequilibrated with 50 mM melibiose ($MelB_{St}$/melibiose complex).

$MelB_{St}$ (Hariharan and Guan, 2014) and LacY (Hariharan et al., 2015) in the absence or presence of galactosides, which corrects the previous notion that $EIIA^{Glc}$ only binds to sugar-bound LacY (Sondej et al., 2002). We have also shown that $EIIA^{Glc}$ inhibits both $MelB_{St}$ and LacY binding affinity for galactosides and suggest that $EIIA^{Glc}$ traps both permeases at outward-open states with low affinity for their sugar substrates (Hariharan and Guan, 2014; Hariharan et al., 2015), which is a key molecular mechanism for the phenomenon called "inducer exclusion." In the current study, the conformational binder $EIIA^{Glc}$ was revisited, and the measurements were extended over all states in the substrate-binding cycle to examine the substrate effects on $MelB_{St}$ conformation.

$EIIA^{Glc}$ binding to the apo $MelB_{St}$ is obtained for the first time, with a K_d value of 4.31 ± 0.84 µM and stoichiometry N number near 1 (Fig. 4 a), which set up a clear reference for analyzing the substrate effects. The apo $MelB_{St}$ sample was preincubated with a saturating concentration of 100 mM NaCl, 50 mM melibiose, or both. $EIIA^{Glc}$ binding to either binary shows little change in affinity and binding stoichiometry. With the $MelB_{St}$–melibiose–Na^+ ternary complex, however, the heat change was largely reduced, which affected the curve-fitting quality. If forcing the stoichiometry N = 1, the estimated K_d value should be fourfold greater than that in the apo state. These changes suggest that $MelB_{St}$ in the ternary favors a conformation that differs from apo, which is consistent with the results from heat capacity and thermostability tests.

Detergent effects exist in several membrane proteins, including the $MelB_{St}$ homologue in *E. coli*, $MelB_{Ec}$ (Amin et al., 2015; Bae et al., 2020). While it has been shown that the detergent UDM is suitable for $MelB_{St}$ functional studies in solution (Guan et al., 2011; Amin et al., 2014; Amin et al., 2015; Hariharan and Guan, 2017), $MelB_{St}$ was reconstituted into lipid nanodiscs to restore the native lipids environment and subjected to $EIIA^{Glc}$-binding measurements (Fig. 4 b). In general, consistent results were obtained, except for a slightly greater heat release in the lipid environment with $EIIA^{Glc}$ binding to $MelB_{St}$ at the ternary state than that in UDM.

Discussion

Extensive structural and functional studies in the past decades have clearly shown that membrane transporters use different types of alternating access to facilitate the translocation of solutes across membranes (Guan and Kaback, 2006; Reyes et al., 2009; Yan, 2015; Kaback and Guan, 2019). The alternating-access process in MFS members involves switching its two -helical bundles between outward- and inward-facing conformations around the substrate-binding site to generate outward- and inward-open solvent-accessing pathways in a cyclical fashion. Between the two states, occluded or several partially occluded intermediates should also coexist. Each transporter might have its favored resting state, such as $MelB_{St}$ favoring outward-open conformations (Ethayathulla et al., 2014) and

Table 2. **Temperature dependence of substrate binding**

Titrant	Titrand (cell)	T (°C)	Test number	K_d (mM)	Free energy change (Δ*G*; kJ/mol)	P	Δ*H* (kJ/mol)	Entropy change (−*T*Δ*S*; kJ/mol)	ΔC_p (J/mol·K)
Mel	$MelB_{St}$ /	15	2	9.15 ± 1.06[a]	−11.27 ± 0.27	>0.05[b]	−25.91 ± 4.58	14.64 ± 4.30	+ 643.01 ± 26.92
		20	2	9.59 ± 1.01	−11.34 ± 0.26		−23.26 ± 5.23	11.92 ± 4.97	
		25	2	10.82 ± 2.49	−11.29 ± 0.58		−19.64 ± 6.13	8.35 ± 6.71	
		30	2	13.79 ± 1.18	−10.81 ± 0.22		−16.40 ± 5.45	5.59 ± 5.66	
Na^+	$MelB_{St}$ /	15	2	0.51 ± 0.08	-18.18 ± 0.39	>0.05	−35.75 ± 0.90	17.56 ± 1.30	+1,305.20 ± 50.63
		20	2	0.60 ± 0.10	−18.13 ± 0.49		−28.20 ± 0.43	10.06 ± 0.02	
		25	2	0.59 ± 0.12	−18.46 ± 0.42		−22.11 ± 0.80	3.65 ± 0.31	
		30	2	0.79 ± 0.07	−18.00 ± 0.22		−16.02 ± 1.40	−1.98 ± 1.62	
Mel	$MelB_{St}$ Na^+	15	3	1.05 ± 0.01	−16.43 ± 0.03	>0.05	−6.46 ± 0.43	−9.61 ± 0.67	− 424.93 ± 40.78
		20	3	0.95 ± 0.13	−17.09 ± 0.40		−9.72 ± 0.59	−7.37 ± 0.99	
		25	5	1.18 ± 0.01	−16.71 ± 0.03		−11.97 ± 0.23	−4.75 ± 0.26	
		30	3	1.41 ± 0.04	−16.55 ± 0.07		−13.57 ± 0.24	−2.98 ± 0.31	
		35	2	1.78 ± 0.14	−16.23 ± 0.20		−15.16 ± 0.44	−1.09 ± 0.23	
Na^+	$MelB_{St}$ Mel	15	2	0.06 ± 0.01	−23.29 ± 0.20	>0.05	−10.70 ± 0.06	−12.59 ± 0.26	−760.50 ± 33.18
		20	2	0.07 ± 0.01	-23.24 ± 0.17		−15.14 ± 0.15	−8.11 ± 0.03	
		25	2	0.12 ± 0.04	−22.55 ± 0.82		−18.74 ± 0.80	−3.82 ± 0.03	
		30	2	0.12 ± 0.03	−22.95 ± 0.74		−22.17 ± 0.52	0.78 ± 1.26	

[a]SEM.
[b]Within each temperature set, the smallest and largest number were used for unpaired *t* test (P > 0.05, no statistical significance among the temperatures).

LacY favoring inward-open conformations (Guan et al., 2007; Smirnova et al., 2011), and these proteins may also undergo a slow time-scale–dependent equilibration with several other states at minor fractions.

The alternating-access process only describes the change in conformation required to deliver the carrying solute to the opposite surface of the protein. Transport process must be dictated or regulated by substrate recognition to assure the specificity of the transporters; in other words, substrate binding should be the mechanism to initiate the alternating-access process. Many transporters, such as uniporters and ABC transporters, only have one type of transported substrate, but cation-coupled symporters have two types of substrate being translocated concurrently. The questions are which substrate (one or both) triggers the conformational changes and initiates transport process, and how the transporters prevent futile transport or cation leak. In this study, we used the Na^+-coupled $MelB_{St}$, a member of MFS transporters, to explore these questions using three different approaches.

Temperature dependence of the $MelB_{St}$ denaturation was analyzed by CD spectroscopy. Interestingly, individual and cooperative effects of Na^+ and melibiose on the thermostability of $MelB_{St}$ exist; i.e., the increase in T_m in the presence of both substrates is greater than the sum from each (Table 1). The substrate-induced increase in thermostability correlates well with the substrate-binding affinity. Structurally, the binding of sugar and/or Na^+ connects and stabilizes multiple helices and charged residues. With the ternary complex, $MelB_{St}$ is likely

Table 3. **Parameterization of entropy change**

Titrant (syringe)	Titrand (cell)		ΔC_p (J/mol·K)	$-\Delta S_{Sum}$ at °25 C (J/mol·K)	$-\Delta S_{Mix}$ (J/mol·K)	$-\Delta S_{Solv}$ (J/mol·K)	$-\Delta S_{Conf}$ (J/mol·K)
Mel	$MelB_{St}$	/	643.01	28.41	33.00	164.61	−169.20
Na^+	$MelB_{St}$	/	1305.20	12.24	33.00	334.13	−354.89
Mel	$MelB_{St}$	Na^+	−424.93	−15.92	33.00	−108.78	59.86
Na^+	$MelB_{St}$	Mel	−760.50	−12.82	33.00	−194.56	148.74

Calculation of each parameter is described in Materials and methods. $-\Delta S_{Sum} = -T\Delta S/298.15$ as measured at 25°C in Table 2.

packed tighter, with stronger interhelical packing. The observation from the two different techniques on positive cooperativities suggests that $MelB_{St}$ conformation in the ternary state might be significantly different from that in the binary and apo states, likely in more closed conformation (such as occluded or partially occluded conformations). A compact conformation for the ternary complex has been suggested by a previous Trp → dansyl galactoside FRET study in $MelB_{Ec}$ and $MelB_{St}$ (Maehrel et al., 1998; Guan et al., 2011), where a stronger FRET intensity in the presence of both ligands was obtained. It is noteworthy that the Trp → dansyl galactoside FRET requires the presence of a galactoside (dansyl galactoside), so no information can be gained from Na^+ binding to apo MelB.

The study with the cation mutant D55C $MelB_{St}$, which does not bind Na^+, revealed interesting results. This cation mutant did not show Na^+-specific stabilizing effects or Na^+ and melibiose cooperative effects as expected. Unexpectedly, this mutant was more stable than the WT; furthermore, Na^+, behaving like the nonsubstrate K^+, only facilitated denaturation at temperatures >53°C. This nonspecific salt effect is also observed with the WT $MelB_{St}$ at high temperatures (>60°C). In general, at high

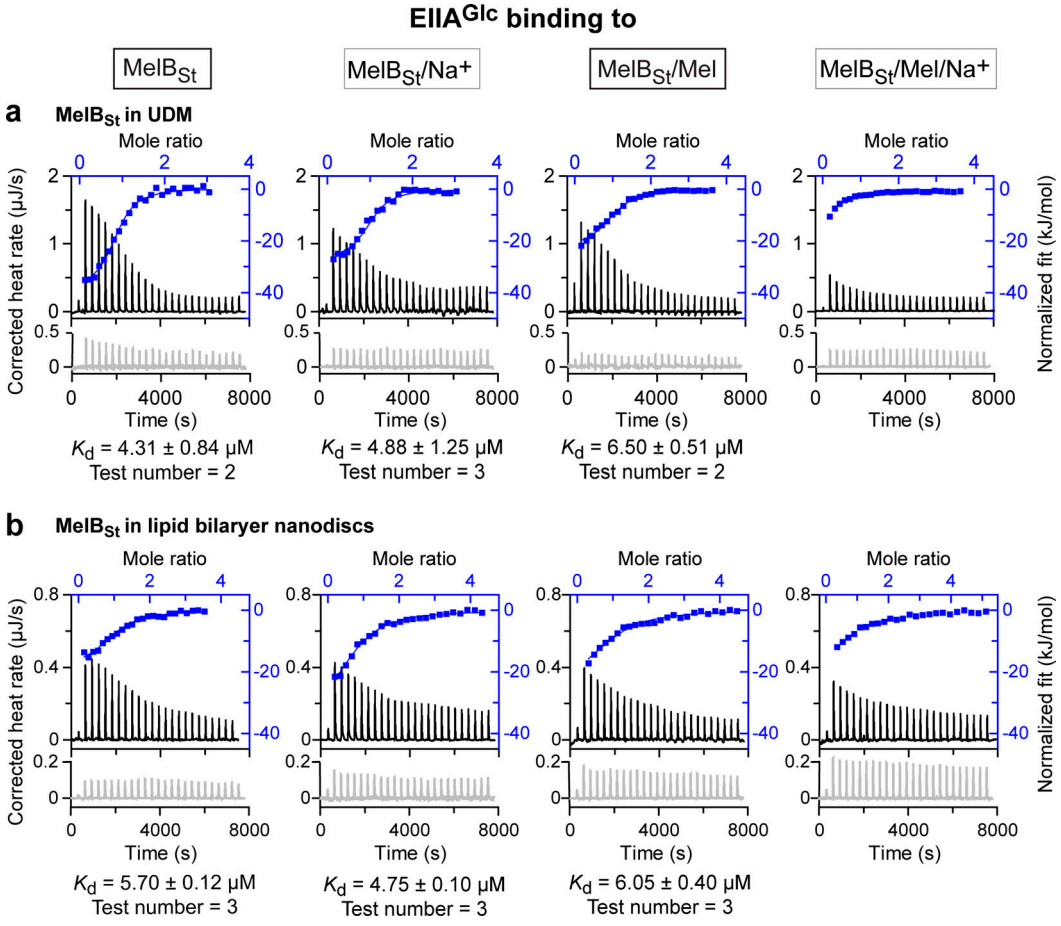

Figure 4. **Substrate effects on $EIIA^{Glc}$ binding to $MelB_{St}$ by ITC.** $EIIA^{Glc}$-binding experiments were conducted at 25°C with the sample cell containing $MelB_{St}$. The thermogram was plotted as the corrected heat rate (μJ/s; left axis) versus time (bottom axis) for the titrant to $MelB_{St}$ (black) or buffer (gray) under an identical scale. **(a)** $EIIA^{Glc}$ injected into $MelB_{St}$ in UDM at 50 μM. **(b)** $EIIA^{Glc}$ injected $MelB_{St}$ in nanodiscs at 20 μM. $EIIA^{Glc}$ binding was measured in four different conditions. From right to left, $MelB_{St}$ in the main buffer (the apo $MelB_{St}$), $MelB_{St}$ preequilibrated with NaCl at 100 mM ($MelB_{St}/Na^+$ binary complex), $MelB_{St}$ preequilibrated with melibiose at 50 mM ($MelB_{St}$/melibiose binary complex), and $MelB_{St}$ preequilibrated with 50 mM melibiose and 100 mM NaCl ($MelB_{St}$/melibiose/Na^+ ternary complex). The normalized heat change (kJ/mol; filled blue symbol) was plotted against the $EIIA^{Glc}/MelB_{St}$ molar ratio using the top/right axes. The K_d value was obtained by fitting the data using the one-site independent-binding model with a fixed binding stoichiometry N number of 1 (for most data, the curve fitting can yield the N number near 1). For $EIIA^{Glc}$ binding to the ternary complex, a smaller heat change prevents accurate curve fitting, so there is no K_d result presented. The number of tests, mean, and standard error are reported under each panel.

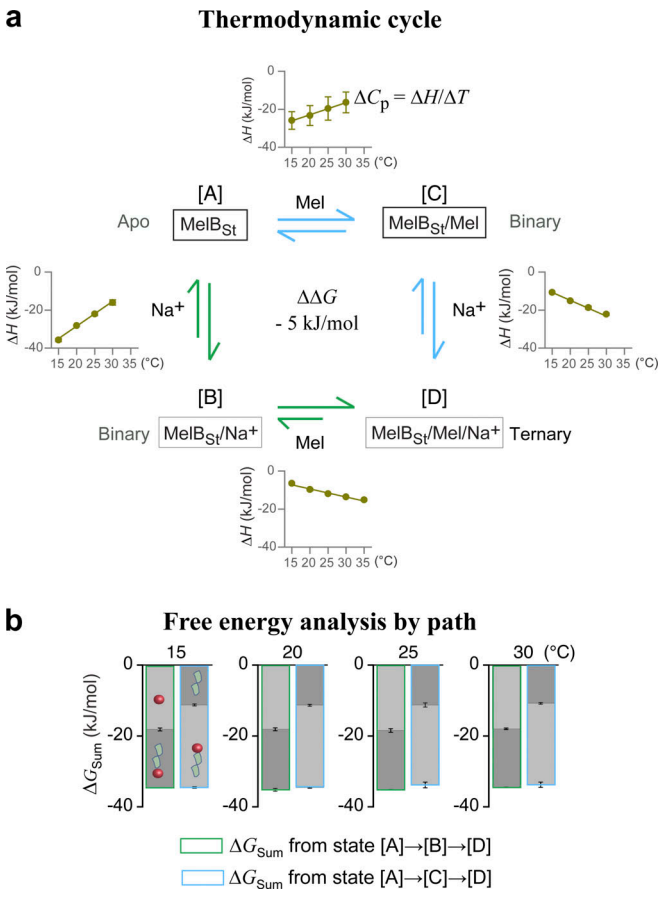

Figure 5. **The binding thermodynamic cycle in MelB$_{St}$. (a)** Thermodynamic cycle of melibiose (Mel) and Na^+ binding to MelB$_{St}$. A four-state model includes the apo state with a cavity possibly opening to periplasmic side [A], two binary complexes MelB$_{St}$/Na^+ [B] and MelB$_{St}$/melibiose [C] with periplasmic open conformation, and the MelB$_{St}$/melibiose/Na^+ ternary complex [D] with an occluded or partially occluded conformation. $\Delta\Delta G$ = −5 kJ/mol is the coupling energy ($\Delta G_{[C]\to[D]} - \Delta G_{[A]\to[B]}$) or $\Delta G_{[B]\to[D]} - \Delta G_{[A]\to[C]}$. The ΔH versus temperature plot for each binding step is displayed as indicated. **(b)** Energy conservation. The histogram shows that total free energy ΔG_{Sum} derived the ternary complex from the two paths (difference in the binding order) are similar at each temperature. $\Delta G_{Sum\ [A]\to[B]\to[D]}$ (left) = $\Delta G_{Sum\ [A]\to[C]\to[D]}$ (right), all approximately −35 kJ/mol within experimental errors.

temperatures, all inherent bonds are weakened; the hydrogen bonds that stabilize α-helical and salt-bridge interactions involving helical packing/domain interactions are disrupted or partially disrupted, and new hydrogen bonds and ionic interactions are established with surrounding water, salts, or other parts of proteins, thus breaking the helical structures and protein folding. At high temperatures, salts may facilitate the disruption process on these important salt bridges that play important roles in MelB$_{St}$ stability and activities (Amin et al., 2014) through nonspecific effects. These data show that (1) MelB$_{St}$ with an empty cation site is less stable, and removal of a negative charge at this cation pocket (such as D55C mutation) significantly increases the protein stability; and (2) Na^+ in MelB$_{St}$ plays a dual role in the heating denaturation process. At lower temperatures (around T_m), Na^+ has a specific stabilizing effect due to its binding to the cation site; at high temperatures (>60°C), it exhibits a nonspecific destabilizing effect that facilitates protein denaturation.

We further characterized the temperature dependence of binding ΔH with ITC on each binding step in the simplified thermodynamic cycle as proposed in Fig. 5 a. It is noteworthy that at each temperature, the thermodynamic cycle is conserved; i.e., the total ΔG derived from the ternary complex is independent of the order of binding (Fig. 5 b). These new data repeatedly confirmed the conclusion on the positive binding cooperativity. Based on the enthalpy–temperature plot (Fig. 5 a), clearly, formation of either binary complex [B] or [C] yields a positive term in ΔC_p, and the formation of a ternary complex [D] yields a negative sign. While the absolute ΔC_p value might not be accurately determined due to technical limitations, the sign should be reliable. For a better understanding of ΔC_p, the entropy term was parameterized. A positive ΔC_p yields a positive sign of $-\Delta S_{Solv}$ (Table 3), meaning that a significant amount of water molecules are dynamically restricted, which can be interpreted as MelB$_{St}$ hydration with cavity opening. Hydration is only observed with a MelB$_{St}$ binary complex. Keep in mind that the binding of sugar or Na^+ with protein requires dehydration of these ion or sugar molecules as well as the MelB$_{St}$ side chains in the binding site, which is a process opposite of hydration. On the other hand, these water molecules released into the MelB$_{St}$ cavity may not gain much entropy freedom due to the confined space. It has also been demonstrated that the water molecules within the SecY translocon are different from bulk water because they are dynamically retarded (Capponi et al., 2015). Nevertheless, the determined value reflects a net hydration effect after compensating the dehydration from ligand binding per se. From a structural point of view, MelB$_{St}$ cavity opening can interpret the hydration process well, suggesting that one substrate binding induces MelB$_{St}$ opening. Under our experimental setup, it is likely that the binding leads to the periplasmic cavity with a lager wet surface and/or with more trapped water molecules. This conclusion is supported by the EIIA^{Glc} binding as explained in a later paragraph.

The negative sign in ΔC_p and $-\Delta S_{Solv}$ suggests a dominated dehydration process, which frees water molecules and increases entropy. While binding of the second substrate molecules also involves dehydration, the value in $-\Delta S_{Solv}$ is much greater, suggesting conformation closure. This interpretation is supported from the thermal denaturation tests (Table 1) and Trp → dandyl galactoside FRET measurements (Maehrel et al., 1998; Guan et al., 2011). Both tests suggest a more compact conformation induced by the cooperative binding of Na^+ and melibiose. There are several studies on other symporters also clearly showing that the binding of cation keeps symporters at open conformation and its transported substrate induces conformation closure, such as the H^+-coupled LacY (Smirnova et al., 2007) and Na^+-coupled glutamate transporter (Focke et al., 2011; Erkens et al., 2013; Hänelt et al., 2013; Arkhipova et al., 2020). It has also been indicated that the high-affinity site for galactoside binding is at an occluded intermediate in LacY (Kumar et al., 2014; Kaback and Guan, 2019).

To further test the notion that the conformation of MelB$_{St}$ in the ternary complex differs from the binary, we applied the

conformational binder $EIIA^{Glc}$ to explore the conformation of $MelB_{St}$. As reported, galactosides afford an effect on $EIIA^{Glc}$ binding opposite of protonated LacY and Na^+-bound $MelB_{St}$, facilitating the binding rate in LacY and decreasing the binding affinity in $MelB_{St}$, likely through altering conformational equilibria (Hariharan and Guan, 2014). This dramatic difference observed from two permeases belonging to the same superfamily likely stems from their differences at resting state, with LacY favoring an inward state (Guan et al., 2007) and MelB favoring an outward state (Ethayathulla et al., 2014). It is likely that galactoside binding to the cation-bound MelB or LacY altered their conformational equilibria. In the same study, we also reported (for $MelB_{Ec}$) no sugar effect on $EIIA^{Glc}$ binding (Hariharan and Guan, 2014), but a later study showed that $MelB_{Ec}$ protein in detergent DDM is likely loosely packed and unable to bind melibiose (Amin et al., 2015). Our data also show that the conformational binder $EIIA^{Glc}$ selects for permeases at certain conformations, likely trapping $MelB_{St}$ at outward-open states (Hariharan and Guan, 2014). The substrate binding shifts the conformational equilibrium toward (in LacY) or away from (in $MelB_{St}$) the optimal binding configurations. Thus, the $EIIA^{Glc}$-binding approach seems useful to test permease conformational changes (Hariharan et al., 2015), which can also be a useful tool for many other non-PTS sugar transporters.

In this study, $EIIA^{Glc}$ binds readily to the apo $MelB_{St}$ and Na^+-bound state; with the melibiose-bound state, only a small difference was obtained (Fig. 4), which suggests that the two binary complexes and the apo state likely belong to an outward-open conformational cluster and support the conclusion drawn from ΔC_p studies. To the $MelB_{St}$ ternary complex, $EIIA^{Glc}$ binding is suboptimal, and the stoichiometry number is affected, decreasing from 1 to 0.7, which might also suggest conformational effects. This measurement was also performed with $MelB_{St}$ in lipid nanodiscs, which yields a similar pattern but a smaller change, with $EIIA^{Glc}$ binding to the ternary complex. The $EIIA^{Glc}$-binding site should be located on the cytoplasmic surface, and this allostatic regulatory site is expected to be structurally sensitive to $MelB_{St}$ conformation. At the outward-open apo and Na^+-binary complex (Fig. 4), an intact $EIIA^{Glc}$-binding site is likely formed and readily accessible, but distorted in the ternary complex due to the cooperative binding of both substrates, which strongly supports the notion that $MelB_{St}$ in ternary complex may favor occluded or partially occluded intermediates.

Overall, the cosubstrate binding thermodynamic cycle in $MelB_{St}$ has been systematically investigated with three independent techniques, including thermal denaturation, heat capacity, and a conformational binder. All consistently argue that the apo $MelB_{St}$ is apparently conformationally labile and readily converts to different states, including inward-facing conformations for substrate access. This flexibility is restrained when bound with one substrate, which is then altered by the second substrate binding; thus, the cooperative binding initiates the transport process by triggering conformational changes to occluded intermediates. This regulatory mechanism based on cooperative binding could ensure the obligatory cotransport in $MelB_{St}$, and this should be a general mechanism for all symporters. While this binding study shows that either substrate can bind to $MelB_{St}$ in solution and that a binding order is not necessary, during the transport cycle, an ordered binding still dictates the transport process. There is a large (at least 20-fold) difference in apo $MelB_{St}$ binding affinities between Na^+ (~0.5 mM) and melibiose (~10 mM). Melibiose affinity in the apo state is too low; in addition, more available Na^+ strongly favors this ordered binding mode. As a result, the Na^+-bound MelB with largely increased affinity for sugar will allow the cells to harvest galactosides in sugar-scarce environments.

Acknowledgments

Joseph A. Mindell served as editor.

The authors thank Dr. Guillermo Altenberg, Texas Tech University Health Sciences Center, Lubbock, TX, for providing plasmid pMSP1E3D1 and discussions about nanodisc reconstitution.

This study was supported by the National Institutes of Health (grants R01GM122759 and R21NS105863 to L. Guan).

The authors declare no competing financial interests.

Author contributions: L. Guan conceptualized this work. P. Hariharan performed all data collection. Both analyzed the data. L. Guan wrote the manuscript, with help from P. Hariharan.

Submitted: 18 July 2020
Revised: 7 April 2021
Accepted: 14 May 2021

References

Abramson, J., I. Smirnova, V. Kasho, G. Verner, H.R. Kaback, and S. Iwata. 2003. Structure and mechanism of the lactose permease of *Escherichia coli Science*. 301:610–615. https://doi.org/10.1126/science.1088196

Amin, A., A.S. Ethayathulla, and L. Guan. 2014. Suppression of conformation-compromised mutants of *Salmonella enterica* serovar Typhimurium MelB. *J. Bacteriol.* 196:3134–3139. https://doi.org/10.1128/JB.01868-14

Amin, A., P. Hariharan, P.S. Chae, and L. Guan. 2015. Effect of detergents on galactoside binding by melibiose permeases. *Biochemistry*. 54: 5849–5855. https://doi.org/10.1021/acs.biochem.5b00660

Arkhipova, V., A. Guskov, and D.J. Slotboom. 2020. Structural ensemble of a glutamate transporter homologue in lipid nanodisc environment. *Nat. Commun.* 11:998. https://doi.org/10.1038/s41467-020-14834-8

Bae, H.E., C. Cecchetti, Y. Du, S. Katsube, J.S. Mortensen, W. Huang, S. Rehan, H.J. Lee, C.J. Loland, L. Guan, et al. 2020. Pendant-bearing glucose-neopentyl glycol (P-GNG) amphiphiles for membrane protein manipulation: Importance of detergent pendant chain for protein stabilization. *Acta Biomater.* 112:250–261. https://doi.org/10.1016/j.actbio.2020.06.001

Bassilana, M., E. Damiano-Forano, and G. Leblanc. 1985. Effect of membrane potential on the kinetic parameters of the Na+ or H+ melibiose symport in Escherichia coli membrane vesicles. *Biochem. Biophys. Res. Commun.* 129:626–631. https://doi.org/10.1016/0006-291X(85)91937-0

Capponi, S., M. Heyden, A.N. Bondar, D.J. Tobias, and S.H. White. 2015. Anomalous behavior of water inside the SecY translocon. *Proc. Natl. Acad. Sci. USA.* 112:9016–9021. https://doi.org/10.1073/pnas.1424483112

Damiano-Forano, E., M. Bassilana, and G. Leblanc. 1986. Sugar binding properties of the melibiose permease in Escherichia coli membrane vesicles. Effects of Na+ and H+ concentrations. *J. Biol. Chem.* 261: 6893–6899. https://doi.org/10.1016/S0021-9258(19)62700-6

Deutscher, J., F.M. Aké, M. Derkaoui, A.C. Zébré, T.N. Cao, H. Bouraoui, T. Kentache, A. Mokhtari, E. Milohanic, and P. Joyet. 2014. The bacterial phosphoenolpyruvate:carbohydrate phosphotransferase system: regulation by protein phosphorylation and phosphorylation-dependent protein-protein interactions. *Microbiol. Mol. Biol. Rev.* 78:231–256. https://doi.org/10.1128/MMBR.00001-14

Erkens, G.B., I. Hänelt, J.M. Goudsmits, D.J. Slotboom, and A.M. van Oijen. 2013. Unsynchronised subunit motion in single trimeric sodium-coupled aspartate transporters. *Nature.* 502:119–123. https://doi.org/10.1038/nature12538

Ethayathulla, A.S., M.S. Yousef, A. Amin, G. Leblanc, H.R. Kaback, and L. Guan. 2014. Structure-based mechanism for Na^+/melibiose symport by MelB. *Nat. Commun.* 5:3009. https://doi.org/10.1038/ncomms4009

Focke, P.J., P. Moenne-Loccoz, and H.P. Larsson. 2011. Opposite movement of the external gate of a glutamate transporter homolog upon binding cotransported sodium compared with substrate. *J. Neurosci.* 31:6255–6262. https://doi.org/10.1523/JNEUROSCI.6096-10.2011

Ganea, C., T. Pourcher, G. Leblanc, and K. Fendler. 2001. Evidence for intraprotein charge transfer during the transport activity of the melibiose permease from *Escherichia coli Biochemistry*. 40:13744–13752. https://doi.org/10.1021/bi011223k

Ganea, C., K. Meyer-Lipp, R. Lemonnier, A. Krah, G. Leblanc, and K. Fendler. 2011. G117C MelB, a mutant melibiose permease with a changed conformational equilibrium. *Biochim. Biophys. Acta.* 1808:2508–2516. https://doi.org/10.1016/j.bbamem.2011.07.017

Granell, M., X. León, G. Leblanc, E. Padrós, and V.A. Lórenz-Fonfría. 2010. Structural insights into the activation mechanism of melibiose permease by sodium binding. *Proc. Natl. Acad. Sci. USA.* 107:22078–22083. https://doi.org/10.1073/pnas.1008649107

Guan, L. 2018. Encyclopedia of Biophysics. Second edition. G. Roberts, and A. Watts, editors. Springer, Berlin. 2807 pp.

Guan, L., and H.R. Kaback. 2006. Lessons from lactose permease. *Annu. Rev. Biophys. Biomol. Struct.* 35:67–91. https://doi.org/10.1146/annurev.biophys.35.040405.102005

Guan, L., O. Mirza, G. Verner, S. Iwata, and H.R. Kaback. 2007. Structural determination of wild-type lactose permease. *Proc. Natl. Acad. Sci. USA.* 104:15294–15298. https://doi.org/10.1073/pnas.0707688104

Guan, L., S. Nurva, and S.P. Ankeshwarapu. 2011. Mechanism of melibiose/cation symport of the melibiose permease of *Salmonella typhimurium* *J. Biol. Chem.* 286:6367–6374. https://doi.org/10.1074/jbc.M110.206227

Gwizdek, C., G. Leblanc, and M. Bassilana. 1997. Proteolytic mapping and substrate protection of the *Escherichia coli* melibiose permease. *Biochemistry*. 36:8522–8529. https://doi.org/10.1021/bi970312n

Hänelt, I., D. Wunnicke, E. Bordignon, H.J. Steinhoff, and D.J. Slotboom. 2013. Conformational heterogeneity of the aspartate transporter Glt(Ph). *Nat. Struct. Mol. Biol.* 20:210–214. https://doi.org/10.1038/nsmb.2471

Hariharan, P., and L. Guan. 2014. Insights into the inhibitory mechanisms of the regulatory protein IIA(Glc) on melibiose permease activity. *J. Biol. Chem.* 289:33012–33019. https://doi.org/10.1074/jbc.M114.609255

Hariharan, P., and L. Guan. 2017. Thermodynamic cooperativity of cosubstrate binding and cation selectivity of *Salmonella typhimurium* MelB. *J. Gen. Physiol.* 149:1029–1039. https://doi.org/10.1085/jgp.201711788

Hariharan, P., D. Balasubramaniam, A. Peterkofsky, H.R. Kaback, and L. Guan. 2015. Thermodynamic mechanism for inhibition of lactose permease by the phosphotransferase protein IIAGlc. *Proc. Natl. Acad. Sci. USA.* 112:2407–2412. https://doi.org/10.1073/pnas.1500891112

Hariharan, P., E. Tikhonova, J. Medeiros-Silva, A. Jeucken, M.V. Bogdanov, W. Dowhan, J.F. Brouwers, M. Weingarth, and L. Guan. 2018. Structural and functional characterization of protein-lipid interactions of the Salmonella typhimurium melibiose transporter MelB. *BMC Biol.* 16:85. https://doi.org/10.1186/s12915-018-0553-0

Huang, Y., M.J. Lemieux, J. Song, M. Auer, and D.N. Wang. 2003. Structure and mechanism of the glycerol-3-phosphate transporter from *Escherichia coli Science*. 301:616–620. https://doi.org/10.1126/science.1087619

Kaback, H.R. 2015. A chemiosmotic mechanism of symport. *Proc. Natl. Acad. Sci. USA.* 112:1259–1264. https://doi.org/10.1073/pnas.1419325112

Kaback, H.R., and L. Guan. 2019. It takes two to tango: The dance of the permease. *J. Gen. Physiol.* 151:878–886. https://doi.org/10.1085/jgp.201912377

Kumar, H., V. Kasho, I. Smirnova, J.S. Finer-Moore, H.R. Kaback, and R.M. Stroud. 2014. Structure of sugar-bound LacY. *Proc. Natl. Acad. Sci. USA.* 111:1784–1788. https://doi.org/10.1073/pnas.1324141111

Lopilato, J., T. Tsuchiya, and T.H. Wilson. 1978. Role of Na+ and Li+ in thiomethylgalactoside transport by the melibiose transport system of Escherichia coli. *J. Bacteriol.* 134:147–156. https://doi.org/10.1128/JB.134.1.147-156.1978

Maehrel, C., E. Cordat, I. Mus-Veteau, and G. Leblanc. 1998. Structural studies of the melibiose permease of *Escherichia coli* by fluorescence resonance energy transfer. I. Evidence for ion-induced conformational change. *J. Biol. Chem.* 273:33192–33197. https://doi.org/10.1074/jbc.273.50.33192

Meadow, N.D., and S. Roseman. 1982. Sugar transport by the bacterial phosphotransferase system. Isolation and characterization of a glucose-specific phosphocarrier protein (IIIGlc) from Salmonella typhimurium. *J. Biol. Chem.* 257:14526–14537. https://doi.org/10.1016/S0021-9258(19)45410-0

Meyer-Lipp, K., N. Séry, C. Ganea, C. Basquin, K. Fendler, and G. Leblanc. 2006. The inner interhelix loop 4-5 of the melibiose permease from *Escherichia coli* takes part in conformational changes after sugar binding. *J. Biol. Chem.* 281:25882–25892. https://doi.org/10.1074/jbc.M601259200

Mus-Veteau, I., and G. Leblanc. 1996. Melibiose permease of *Escherichia coli*: structural organization of cosubstrate binding sites as deduced from tryptophan fluorescence analyses. *Biochemistry*. 35:12053–12060. https://doi.org/10.1021/bi961372g

Mus-Veteau, I., T. Pourcher, and G. Leblanc. 1995. Melibiose permease of *Escherichia coli*: substrate-induced conformational changes monitored by tryptophan fluorescence spectroscopy. *Biochemistry*. 34:6775–6783. https://doi.org/10.1021/bi00020a024

Niiya, S., Y. Moriyama, M. Futai, and T. Tsuchiya. 1980. Cation coupling to melibiose transport in *Salmonella typhimurium J. Bacteriol.* 144:192–199. https://doi.org/10.1128/JB.144.1.192-199.1980

Poolman, B., J. Knol, C. van der Does, P.J. Henderson, W.J. Liang, G. Leblanc, T. Pourcher, and I. Mus-Veteau. 1996. Cation and sugar selectivity determinants in a novel family of transport proteins. *Mol. Microbiol.* 19:911–922. https://doi.org/10.1046/j.1365-2958.1996.397949.x

Pourcher, T., M. Bassilana, H.K. Sarkar, H.R. Kaback, and G. Leblanc. 1990. The melibiose/Na+ symporter of *Escherichia coli*: kinetic and molecular properties. *Philos. Trans. R. Soc. Lond. B Biol. Sci.* 326:411–423. https://doi.org/10.1098/rstb.1990.0021

Pourcher, T., S. Leclercq, G. Brandolin, and G. Leblanc. 1995. Melibiose permease of Escherichia coli: large scale purification and evidence that H+, Na+, and Li+ sugar symport is catalyzed by a single polypeptide. *Biochemistry*. 34:4412–4420. https://doi.org/10.1021/bi00013a033

Reyes, N., C. Ginter, and O. Boudker. 2009. Transport mechanism of a bacterial homologue of glutamate transporters. *Nature*. 462:880–885. https://doi.org/10.1038/nature08616

Ritchie, T.K., Y.V. Grinkova, T.H. Bayburt, I.G. Denisov, J.K. Zolnerciks, W.M. Atkins, and S.G. Sligar. 2009. Chapter 11-Reconstitution of membrane proteins in phospholipid bilayer nanodiscs. *Methods Enzymol.* 464:211–231. https://doi.org/10.1016/S0076-6879(09)64011-8

Saier, M.H. Jr., J.T. Beatty, A. Goffeau, K.T. Harley, W.H. Heijne, S.C. Huang, D.L. Jack, P.S. Jähn, K. Lew, J. Liu, et al. 1999. The major facilitator superfamily. *J. Mol. Microbiol. Biotechnol.* 1:257–279.

Smirnova, I., V. Kasho, J.Y. Choe, C. Altenbach, W.L. Hubbell, and H.R. Kaback. 2007. Sugar binding induces an outward facing conformation of LacY. *Proc. Natl. Acad. Sci. USA.* 104:16504–16509. https://doi.org/10.1073/pnas.0708258104

Smirnova, I., V. Kasho, and H.R. Kaback. 2011. Lactose permease and the alternating access mechanism. *Biochemistry*. 50:9684–9693. https://doi.org/10.1021/bi2014294

Sondej, M., A.B. Weinglass, A. Peterkofsky, and H.R. Kaback. 2002. Binding of enzyme IIAGlc, a component of the phosphoenolpyruvate:sugar phosphotransferase system, to the Escherichia coli lactose permease. *Biochemistry*. 41:5556–5565. https://doi.org/10.1021/bi011990j

Tsuchiya, T., and T.H. Wilson. 1978. Cation-sugar cotransport in the melibiose transport system of *Escherichia coli Membr. Biochem.* 2:63–79. https://doi.org/10.3109/09687687809063858

Turnbull, W.B., and A.H. Daranas. 2003. On the value of c: can low affinity systems be studied by isothermal titration calorimetry? *J. Am. Chem. Soc.* 125:14859–14866. https://doi.org/10.1021/ja036166s

Wilson, T.H., and P.Z. Ding. 2001. Sodium-substrate cotransport in bacteria. *Biochim. Biophys. Acta*. 1505:121–130. https://doi.org/10.1016/S0005-2728(00)00282-6

Wilson, D.M., and T.H. Wilson. 1987. Cation specificity for sugar substrates of the melibiose carrier in *Escherichia coli Biochim. Biophys. Acta*. 904:191–200. https://doi.org/10.1016/0005-2736(87)90368-3

Yan, N. 2015. Structural biology of the major facilitator superfamily transporters. *Annu. Rev. Biophys.* 44:257–283. https://doi.org/10.1146/annurev-biophys-060414-033901

Zakariassen, H., and M. Sorlie. 2007. Heat capacity changes in heme protein-ligand interactions. *Thermochim. Acta*. 464:24–28. https://doi.org/10.1016/j.tca.2007.07.021

Zoghbi, M.E., R.S. Cooper, and G.A. Altenberg. 2016. The lipid bilayer modulates the structure and function of an ATP-binding cassette exporter. *J. Biol. Chem.* 291:4453–4461. https://doi.org/10.1074/jbc.M115.698498